Efficiency Approximation of Centrifugal Compressors in the Cordier-Diagram

Y. Lattner [A,*] *- M. Geller* [A] *- N. Kluck* [A]

[A]University of Applied Sciences and Arts Dortmund, Faculty of Mechanical Engineering
[*]Corresponding author E-Mail: yannick.lattner@fh-dortmund.de

ABSTRACT

We present a simulation data-based efficiency approximation for radial turbocompressors, which is implemented in the well-known Cordier diagram. A sophisticated *CAE* workflow is used to calculate the operational characteristics of 50 machine designs with 50 impeller geometry variations each. A Kriging-based surrogate model is trained to approximate the efficiency of any machine designs' best geometry design. The models are implemented into a machine design workflow. As a result, duty-specific Cordier lines are introduced. They are automatically generated for a set of machine design parameters. The efficiency of the designs along the duty-specific Cordier lines is approximated. Using optimization techniques, an optimal compressor design for the given duty on every specific Cordier line may be identified. This highly increases the amount of information available in the early design stages for radial turbocompressors.

KEYWORDS

CENTRIFUGAL COMPRESSOR, CORDIER DIAGRAM, CFD, METAMODELING, DESIGN OF EXPERIMENTS

NOMENCLATURE

LATIN SYMBOLS

c	Velocity in $\mathrm{m\,s^{-1}}$
	Chord length in m
D	Diameter in m
L	Impeller length in m
$\dot{m}$	Mass flow in $\mathrm{kg\,s^{-1}}$
n	Rotational velocity in $1/\mathrm{s}$
p	Pressure in Pa
Re	Reynold's number
T	Temperature in K
u	Circumferential velocity in $\mathrm{m\,s^{-1}}$
$\dot{V}$	Volume flow $\mathrm{m^3\,s^{-1}}$
w	Relative velocity in $\mathrm{m\,s^{-1}}$
y	Technical work $\mathrm{J\,s^{-1}}$
y^+	Non-dimensional wall distance
z	Number of blades

GREEK SYMBOLS

β	Relative blade angle in $^\circ$
δ	Specific diameter
η	Efficiency
θ	Circumferential blade angle in $^\circ$
ν	Kinematic viscosity in $\mathrm{m^2\,s^{-1}}$
	Geometric ratio
Π	Pressure ratio
σ	Specific speed
φ_D	Flow coefficient

SUBSCRIPTS

Pol	Polytropic
s	Static conditions
t	Total conditions
Op	Operational Point

INTRODUCTION

The design process of centrifugal compressors has become increasingly complex. Both the compressor and its development must be efficient. Therefore, a streamlined process — using as few as possible design iterations, simulations, and prototypes — is necessary.

At the beginning of calculating the centrifugal compressor's principal dimensions, the future machine's efficiency is estimated using correlations models (e.g., Rodgers (1979), C. Rodgers (1991), and Rusch and Casey (2012)). As very little information is present at this time, those correlations are empirical models, requiring very few input parameters.

Next, the Cordier line (Cordier 1953) is used to find an impeller diameter D_2 for a chosen rotational speed n or vice versa. This is possible because the Cordier diagram's data is plotted using the non-dimensional numbers specific speed σ (Equation 1) and the specific diameter δ (Equation 2), which depend solely on either impeller diameter D_2 or rotational speed n:

$$\sigma = \frac{n \cdot \sqrt{\dot{V}_0}}{y^{\frac{3}{4}}} \left(2\pi^2\right)^{\frac{1}{4}} \qquad (1)\ , \qquad \delta = \frac{D_2 \cdot y^{\frac{1}{4}}}{\sqrt{\dot{V}_0}} \left(\frac{\pi^2}{8}\right)^{\frac{1}{4}} \qquad (2)$$

This procedure is based on the assumption, that centrifugal compressors on the Cordier line feature good efficiency in contrast to compressors away from the Cordier line. Cordier — however — states that radial machines coincide much more closely than axial ones, and that "lines of constant efficiency cannot be specified here with similar success." (Cordier 1953). This suggests that the original Cordier diagram never intended to provide any kind of efficiency approximation for radial machines. Thus, the Cordier line does not specify where high-efficiency centrifugal compressor are within the Cordier diagram, rather than indicating where those machines may be designed at all.

Additionally, modern centrifugal compressors differ greatly from those available in 1953. Modern machines are no longer limited to radial ending blades and feature complex, twisted blade distributions. Cordier describes such a design for pumps. He states that compressors may not be built the same way (Cordier 1953). Thus, centrifugal compressors similar to today's designs have not been considered in the original Cordier diagram.

Even more, while defining the machine's properties, some parameters are iterated to ensure that the design is capable of providing the required mass flow and pressure rise. These adaptions change the compressor design's location within the Cordier diagram. This can be observed for designs, which have been optimized to optimum efficiency. As principal properties of the compressor are fixed for most optimization processes (e.g, Geller et al. (2017), Kim et al. (2010), and Omidi et al. (2019)), the machine's characteristic is not iterated. For compressor developments, which included the machine's principal dimension in the optimization process, a deviation of the final design from the original Cordier line could be identified (e.g., Giuffre et al. (2022), and Schemmann (2019)). Giuffre et al. (2022) also identified an optimum compressor design away from the Cordier line, which they would not have been identified by using a Cordier line-based design process. All this indicates, that fixing the machine characteristics using the Cordier diagram – without further information — may prevent the designer from identifying more efficient machine designs for a given duty.

This study seeks to overcome this issue by creating a surrogate model, which approximates the efficiency of radial turbocompressors in the Cordier diagram. The location of modern designs inside the Cordier diagram is discussed in the next section. Then, a two-level design of experiments *(DoE)*, which features 50 machine designs and — for each of those machine designs — 50 geometry variations and the calculation of the speed lines for all 2,500 designs

is described. An efficiency-approximating surrogate model's training and implementation in a machine design workflow is presented next. Duty-specific Cordier lines are introduced as a method to re-enable the use of the Cordier line's concept. Finally, a conclusion is given.

MULTI-LEVEL DESIGN SPACE

To provide an efficiency approximation within the Cordier diagram, only parameters available at the beginning of the design process can be used. Influences, which are introduced by the specific geometry design, have to be filtered. The parameter set is thus divided into two levels: Machine design and geometry design.

Level 1: Machine Design

The machine design defines the radial compressor's principal dimensions and energetic properties. A design point generated within this parameter space is labeled *machine design point* (`mDP`). The machine design of the centrifugal compressors is generated using a MATLAB tool, in which, the design workflow by Fister (1986) has been implemented. The necessary efficiency approximation is done using the equations provided by Rusch and Casey (2012). To obtain a valid design, equity of the impeller's geometric work and the required thermodynamic work must be ensured by adapting design parameters. In this study, the rotational speed n is iterated.

An equal sample distribution along the Cordier line is ensured by the parameter *Cordier line position*. It defines the design's sampling location along the Cordier line and can thus be directly converted into a data pair of specific speed σ and specific diameter δ.

All parameters available for defining the machine design are listed below:

Table 1: List of machine design parameters.

Parameter	**Symbol**	**Unit**	**DoE Properties**	
Sampled properties			*Range*	
Cordier line position	s_{CORDIER}	-	0	1
Outflow pressure	p_{Out}	Pa	2×10^5	4×10^5
Ambient volume flow	$\dot{V}_{\mathrm{Amb}}$	$\mathrm{m^3\,s^{-1}}$	0.5	4
Axial impeller extent ratio	ν_L	-	0.2	0.4
Trailing edge blade angle	β_2	°	40	75
Circumferential blade extent	θ_2	°	35	55
Constant properties			*Value*	
Ambient pressure	p_{Amb}	Pa	1×10^5	
Ambient temperature	T_{Amb}	K	288.15	
Hub to shaft diameter ratio	$D_{1_{\mathrm{Hub}}}/D_{\mathrm{Shaft}}$	-	1.25	
Blade thickness ratio	ν_S	-	0.01	
Number of blades	z	-	13	

Level 2: Geometry Design

The geometry design describes and defines the actual impeller's shape. The geometric design can have a significant influence on the compressor's efficiency while maintaining its overall machine design. A design point generated within this parameter space is labeled *geometry design point* (`gDP`).

The CAD geometry of the impeller is created with the program ANSYS DESIGNMODELER. A turbomachinery's impeller is traditionally defined by its outer diameter D_2. All other parameters are best described in a non-dimensional manner. For length values, this is done by

using the ratio to the outer diameter. These parameters are named ν. The subscript denotes the corresponding dimension.

To define the impeller's hub and shroud contour, Bézier splines are used. The spline's control point's locations are defined within relative, pre-defined boundaries. A reduced parameter set is implemented to minimize the design space's dimensions. For each meridional spline (hub & shroud) only two parameters are used. Those move the splines' control points in streamwise and meridional direction, respectively.

The distribution of the circumferential blade angle θ is also defined using Bézier splines. Within specified limits, the control points are positioned by a single parameter for hub and shroud each. The parameters are designed to drive the intensity of the *S*-shape of the distribution of the relative blade angle β.

Thanks to the non-dimensional definition of all parameters and their standardized ranges (usually 0 to 1 or -1 to 1), the designs of experiments can be defined equal for all machine designs. A list of all geometry design parameters is given below:

Table 2: List of geometry design parameters.

Parameter	**Unit**	**DoE Properties**
Flow path geometry		
Impeller exit diameter	m	*Machine Design*
Number of blades	-	*Machine Design*
Diffuser length ratio	-	*Constant*
Axial impeller extent ratio	-	*Machine Design*
Impeller inlet hub diameter ratio	-	*Machine Design*
Impeller inlet shroud diameter ratio	-	*Machine Design*
Inlet-region length ratio	-	*Constant*
Impeller exit width ratio	-	*Constant*
Diffuser exit width ratio	-	*Constant*
Diffuser pitch length	-	*Constant*
Diffuser pitch depth	-	*Constant*
Hub control points in meridional direction	-	*Sampled*
Hub control points in span wise direction	-	*Sampled*
Shroud control points in meridional direction	-	*Sampled*
Shroud control points in span wise direction	-	*Sampled*
Impeller blade geometry		
Leading edge hub position	-	*Sampled*
Leading edge offset angle hub to shroud	°	*Sampled*
General blade thickness ratio	-	*Machine Design*
Meridional blade thickness ratio	-	*Constant*
Span wise blade thickness ratio	-	*Constant*
Leading edge blade angle on hub	°	*Machine Design*
Leading edge blade angle on shroud	°	*Machine Design*
Trailing edge blade angle	°	*Machine Design*
Trailing edge circumferential blade angle	°	*Machine Design*
Blade twist (Leading edge)	°	*Sampled*
Blade rake (Trailing edge)	°	*Sampled*
Intensity of *S*-shaped theta distribution (Hub)	-	*Sampled*
Intensity of *S*-shaped theta distribution (Shroud)	-	*Sampled*

MODERN COMPRESSORS IN THE CORDIER DIAGRAM

For a given duty of pressure ratio Π and ambient volume flow $\dot{V}_{\mathrm{Amb}}$, the data pair provided by the Cordier diagram leads to values for impeller diameter D_2 and impeller speed n. The before mentioned iteration of the impeller speed to obtain a valid design will change the location of the design within the Cordier diagram. To further understand this movement, a set of 1000 randomly distributed compressor designs is investigated using the first level of the presented design space. The design parameters and their values are given in Table 1.

Being initially located on the Cordier line by the Latin hypercube sampling, the designs are moving away from the Cordier line during the iteration. This can be seen in Figure 1 (a), where every 40th design is shown for improved visibility. The final locations of all 1,000 designs are shown in Figure 1 (b). All designs are found to be inside a stripe rather than on a single line. This stripe may be identified as the area, in which centrifugal compressors — within the parameter bounds used — may be designed. It can be seen, that the designs diverge from the original Cordier Line. For low and high values of specific speed σ, almost no design is on the Cordier line. The relative blade angle β_2 — despite being randomly sampled — shows is a clear influence on the amount of perpendicular offset from the original Cordier line.

All this supports the argument, that more parameters than specific speed σ and specific diameter δ must be used, to describe a centrifugal compressor design location within the Cordier diagram and its efficiency. As shown in Figure 1 (b), the trailing edge's relative blade angle β_2 seems to be a good parameter, to further specify the location of a compressor design within the Cordier diagram.

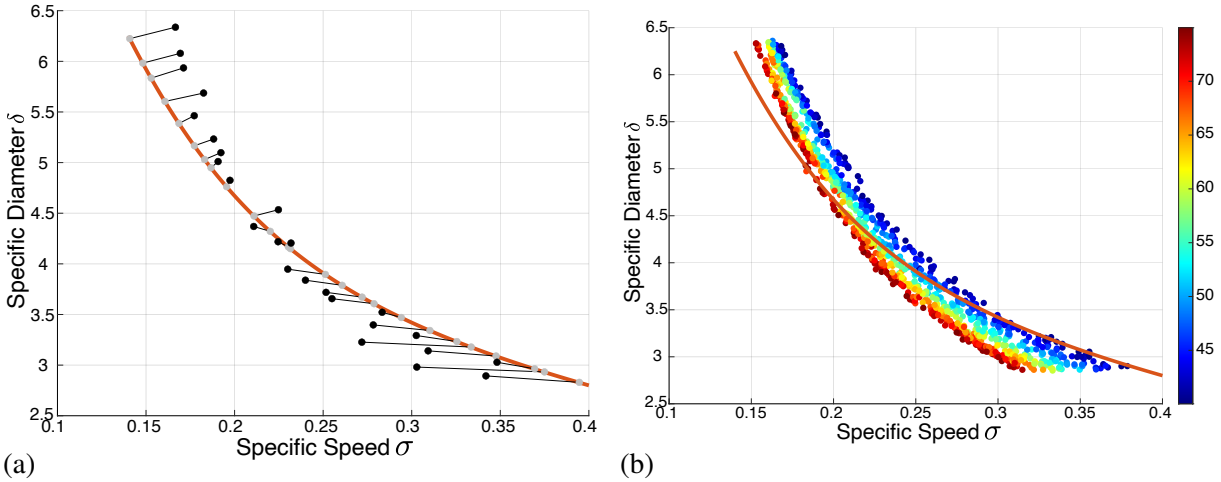

(a) (b)

Figure 1: (a) Movement of the designs within the Cordier diagram. (b) Distribution of machine designs in the Cordier diagram. Color map: Trailing edge relative blade angle β_2.

DESIGN OF EXPERIMENTS

Parameter Sampling

A wide-ranging design of experiments is conducted to obtain efficiency values for a variety of centrifugal compressors using both parameter levels presented. For every single out of 50 machine design points, a set of 50 geometry design points is created. This ensures good coverage of the complete design space.

The 50 machine-design points are created by a Latin hypercube sampling using the parameters and ranges given in Table 1. The distribution of specific speed σ, specific diameter δ within the Cordier diagram — after the design process has been conducted — is shown in Figure 2.

The color map indicated the values for the outflow pressure p_{Out} (Figure 2 (a)) and the ambient volume flow $\dot{V}_{\mathrm{Amb}}$(Figure 2 (b)). It can be seen that those are distributed randomly, even after the designs have been moved during the design process.

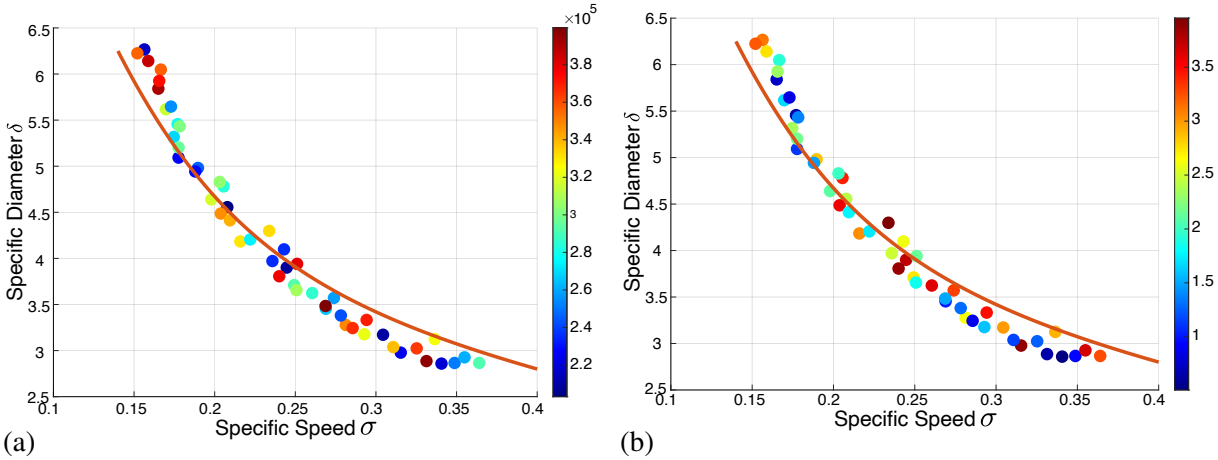

Figure 2: Location of the *DoE* Sampling in the Cordier diagram. The color indicates the value of the outflow pressure in Pa (a) and the ambient volume flow in $\mathrm{m^3\,s^{-1}}$ (b).

For each of those machine design points, 50 geometry design points are generated. The design properties are sampled according to Table 2. The non-dimensional parameter definitions, which are used to define the geometry design, enable the use of the same *LHS*-design for every machine design's geometric design of experiments. Overall, the complete design of experiments contains 2,500 designs, for which the speed line data has to be calculated.

Computational Model

An existing *CFD*-based speed line computation model for centrifugal compressors is employed in this study. It was specifically designed for this task and is described in detail by Lattner et al. (2023). A brief description of the model's principal components is given here.

Mesh

The mesh is generated using ANSYS TURBOGRID. The mesh's topology is automatically defined. A global size factor is used to control the mesh resolution. The first element's thickness is calculated internally by providing a desired value for the non-dimensional wall distance y^+ and the machine's Reynold's number Re. In this study, the chord Reynold's number is used, as it is the most accurate representation of the fluid flow within the impeller (Casey and Robinson 2021). It is defined as $Re_c = {}^{w_1 \cdot c}/_{\nu}$. This approach ensures that the mesh is adapted for every centrifugal compressor within the wide design space of this research. A value of $y^+ = 20$ is observed to provide grid-independent results throughout the design space regarding the accuracy required.

Setup

The *CFD* simulations are conducted using ANSYS CFX. The simulation's setup is designed in accordance to the *CFX Best Practices Guide for Turbomachinery* (Ansys Inc. 2022). A stationary inlet domain, a rotating impeller domain and a stationary, vaneless diffuser domain are employed. The shear stress turbulence model (*SST*) is used.

For evaluating the simulation's convergence, the coefficients of variation — the quotient of standard deviation σ and the mean's absolute $|\mu|$ — is employed: $CV = \sigma/|\mu|$. It is continuously computed on a moving interval of 100 iterations. The mass flow at the inlet $\dot{m}_{\mathrm{In}}$, the total enthalpy rise $\Delta H_{\mathrm{In-Out}}$, and the static outflow Temperature $T_{s_{\mathrm{Out}}}$ are chosen as convergence identifiers. When reaching a threshold value ($CV < 1e-4$) for all identifiers, the simulation is terminated. A second threshold ($CV < 5e-3$) is calibrated to indicate periodically fluctuating results, which are expected for randomly distributed design parameters. In this case, the simulation is not stopped until the penultimate iteration and, for all simulation results, the mean value of the last 100 iterations is used to compensate the periodic behavior.

Speed Line Calculation

The speed line is computed by identifying its most significant points: surge, choke and the operational point: The surge point is identified at the maximum value of the outflow pressure (Cumpsty 1996). The choke point marks a value of mass flow which cannot be exceeded, due to the velocity at the smallest section reaching the local speed of sound (Traupel 2001). The point of maximum efficiency is the operational point, where the compressor would ideally be used.

In operation, the tool automatically starts CFD simulations to scan the speed line at a predefined resolution and identifies the speed line's significant points using optimization algorithms.

All compressor designs were solved by an *HPC*-cluster. Out of the 2,500 designs, only 19 designs have ultimately failed, while for 32 designs, no operational point could be identified. This may happen, if the efficiency does not show a local maximum, but rises all the way to the surge point. This equals an error percentage of 0.76% or 2.08%, respectively.

Results & Post-Processing

To obtain results, which are independent of the resolution of the data provided by the speed line tool, a neural network-based regression technique for speed lines (Lattner et al. 2022) has been used. In this approach, the mass flow $\dot{m}$, the total-to-static pressure ratio $\Pi_{\mathrm{t-s}}$, and the polytropic efficiency η_{Pol} are interpolated as functions of the exit corrected mass flow, which is also used as outlet boundary conditions for all CFD-simulations. All three significant points' coordinates ($\dot{m}$, $\Pi_{\mathrm{t-s}}$ and η_{Pol}) are then calculated using the interpolated data.

The distribution of the maximum efficiency of geometry design within all machine design points is shown in Figure 3. Using the box plot, it can be concluded, that the efficiency depends

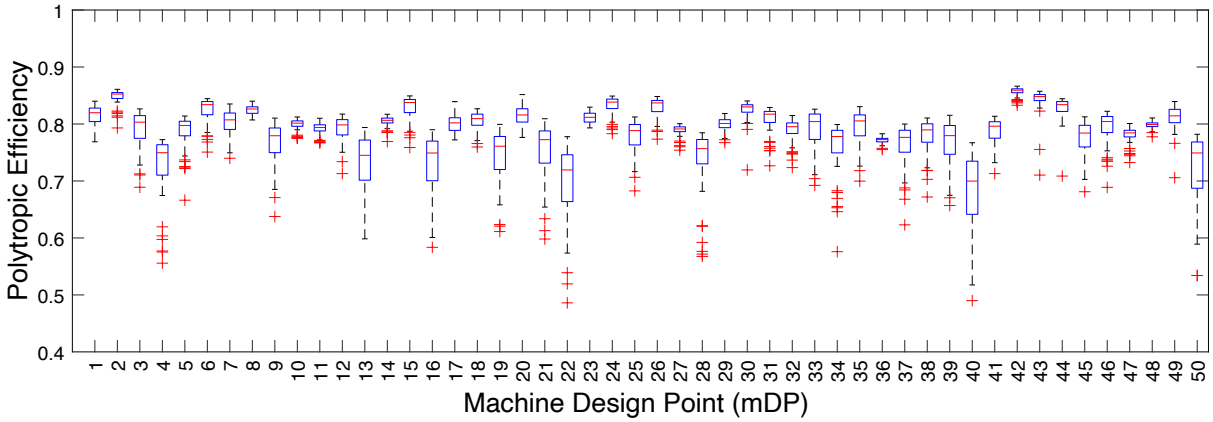

Figure 3: Box plot showing the distribution of the maximum efficiency values within each machine design point.

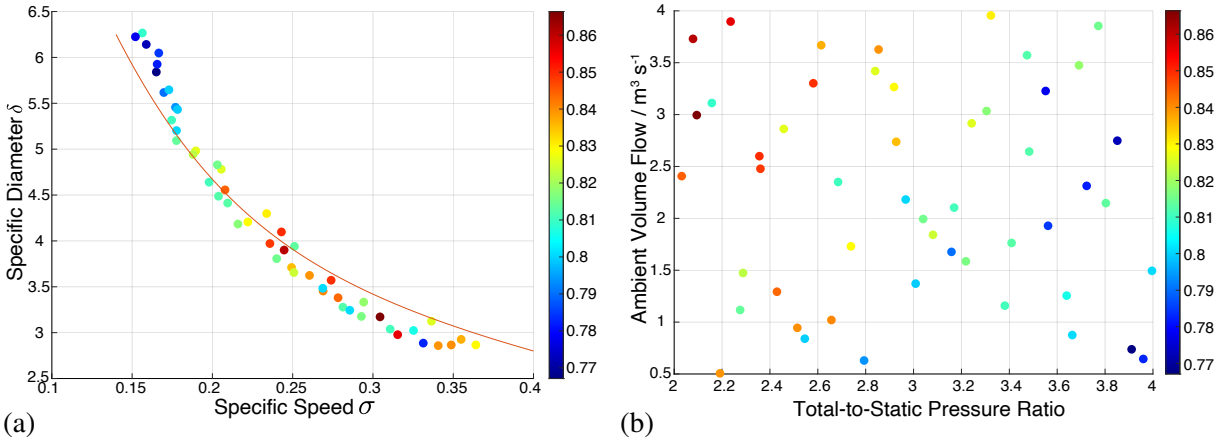

(a) (b)

Figure 4: (a) All machine design points in the Cordier diagram, (b) all machine designs scattered by their design total-to-static pressure ratio $\Pi_{\mathrm{t-s}}$ and ambient volume flow $\dot{V}_{\mathrm{Amb}}$. The color indicated the highest efficiency within the geometry design of experiments.

on both the machine and the geometry design.

For every machine design point, the geometry design point, which features the highest value of efficiency, was identified. These values shall represent the *achievable efficiency* within each machine design point. Figure 4 shows these values. The first plot (a) shows the distribution of those designs in the Cordier diagram. While a low specific speed seems to indicate a lower efficiency, it is evident that the Cordier diagram's parameters are not sufficient to explain the efficiency of centrifugal compressor designs alone. In Figure 4 (b) the design values for total-to-static pressure ratio $\Pi_{\mathrm{t-s}}$ and ambient volume flow $\dot{V}_{\mathrm{Amb}}$ used as axes. Low values of pressure ratios and high values of volume flow seem to produce higher values of efficiency. Still, other parameters' influences are obvious.

EFFICIENCY CORRELATION IN THE CORDIER DIAGRAM

Model Training

To describe the efficiency within the Cordier diagram, multiple parameters are available. In addition to those, which were used to define the machine design points (Table 1), parameters, which can be directly calculated during the machine design process, may be used. Those are specific speed σ and specific diameter δ — directly derived from the Cordier line position s_{CORDIER}, and results from the machine design process: rotational velocity n, impeller diameter D_2, and item impeller tip speed u_2. Additionally, the Chord Reynold's number is employed. This usually requires the actual chord length, which is defined by the geometry design. In this research, a method to approximate the chord length using only machine design parameters by Lattner and Geller (2023) is employed.

To identify parameters, which are sensitive to the efficiency, the software UQLAB's sensitivity analysis tool is employed used (Marelli et al. 2022). The efficiency is found to be significantly sensitive to the following parameters:

- Cordier line position s_{CORDIER}
- Specific speed σ
- Specific diameter δ
- Outflow pressure p_{Out}
- Ambient volume flow $\dot{V}_{\mathrm{Amb}}$
- Axial impeller extent ratio ν_L
- Trailing edge blade angle β_2
- Circumferential blade extent θ_2
- Impeller tip speed u_2

The combination of these parameters — with omission of the *Cordier line position* to avoid redundancy — is used to train a surrogate model. A Kriging implementation provided by the software UQLAB (Lataniotis et al. 2022) is employed. A scanning-test-set cross-validation (STS) as a cross-validation process and a weighted coefficient of determination ($WR2$, Equation 3) is used in model training (Badawy et al. 2017).

$$WR2 = 1 - \frac{SSE_{test} + \alpha SSE_{training}}{SST_{test} + \alpha SST_{training}} \quad \text{with:} \quad \alpha = 0.5 \tag{3}$$

The surrogate model interpolates the simulation data with excellent accuracy: $WR2 = 0.9932$.

Validation

To evaluate the efficiency approximation, it is first compared to a known empirical correlation by Rusch and Casey (2012). The responses of both efficiency approximation models are computed for all 50 machine design points' machine design parameters.

In Figure 5 (a), the efficiency, calculated by both models, is plotted against the flow coefficient φ_D. This non-dimensional number is the reference model's primary variable. In Figure 5 (b), the efficiency values are plotted against the specific speed σ.

In both plots, the correlations show similarities. The overall achievable efficiency is similar. Both models feature a loss of efficiency at low and high values of flow coefficient and specific speed, respectively. However, the consideration of additional input parameters compared to the reference model seems to enable a partial compensation for the loss for low values of flow coefficient and specific speed. This model's data is also more scattered in general. This is expected, as the model has more relevant input parameters. The presented approximation model employs the eight parameters listed above, while the reference model employs — effectively — only requires the ambient volume flow $\dot{V}_{\mathrm{Amb}}$, the impeller tip speed u_2 and the impeller diameter D_2.

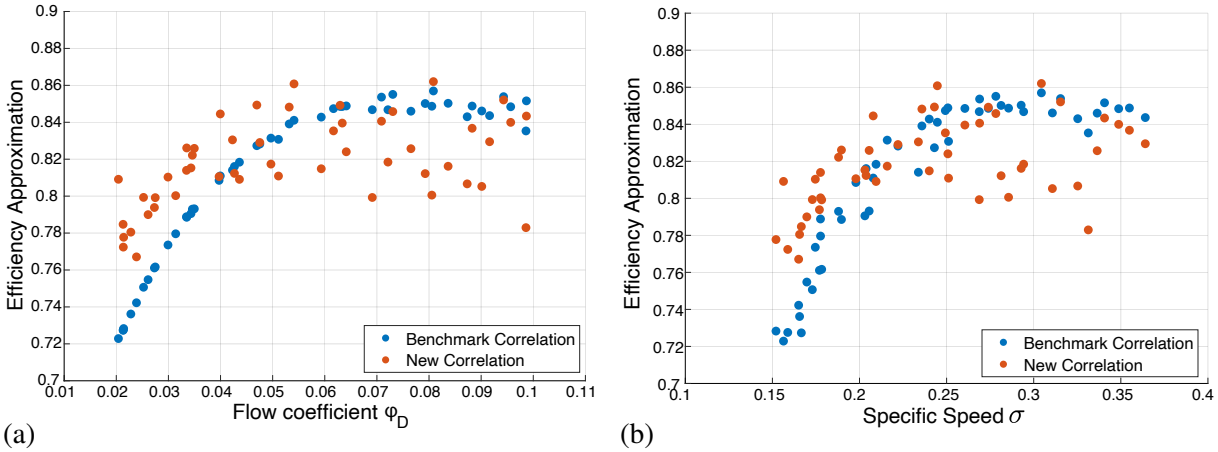

Figure 5: Comparison of a benchmark efficiency correlation (Rusch and Casey 2012) and the presented efficiency correlation. The predicted efficiency value is plotted against the flow parameter φ_D (a) and the specific speed σ (b)

Duty-Specific Cordier Lines

The surrogate model is implemented in the machine design workflow and is thus be used to provide efficiency approximations at the preliminary design stage. But, as seen before, it may not directly be used in the two-dimensional Cordier diagram, due to its complexity. Rather than implementing a universal efficiency approximation into the Cordier diagram, it is more suitable to calculate a set of machine designs along the Cordier line for a defined duty. They are combined to obtain a *duty-specific Cordier line*. On this line, the efficiency approximation is applied. In this study, the procedure is demonstrated using the exemplary duty listed below:

- Outflow pressure $p_{\mathrm{Out}} = 3 \times 10^5\,\mathrm{Pa}$
- Ambient volume flow $\dot{V}_{\mathrm{Amb}} = 2.5\,\mathrm{m^3\,s^{-1}}$
- Axial impeller extent ratio $\nu_L = 0.3$
- Circumferential blade extent $\theta_2 = 40°$

As seen before, the relative blade angle at the trailing edge β_2 has a significant influence on the position within the Cordier diagram. Therefore, four duty-specific Cordier lines are produced for $\beta_2 = 40°,\ 50°,\ 60°$ and $70°$. Figure 6 shows the four duty-specific Cordier lines. The efficiency is approximated for each support point using the trained surrogate model.

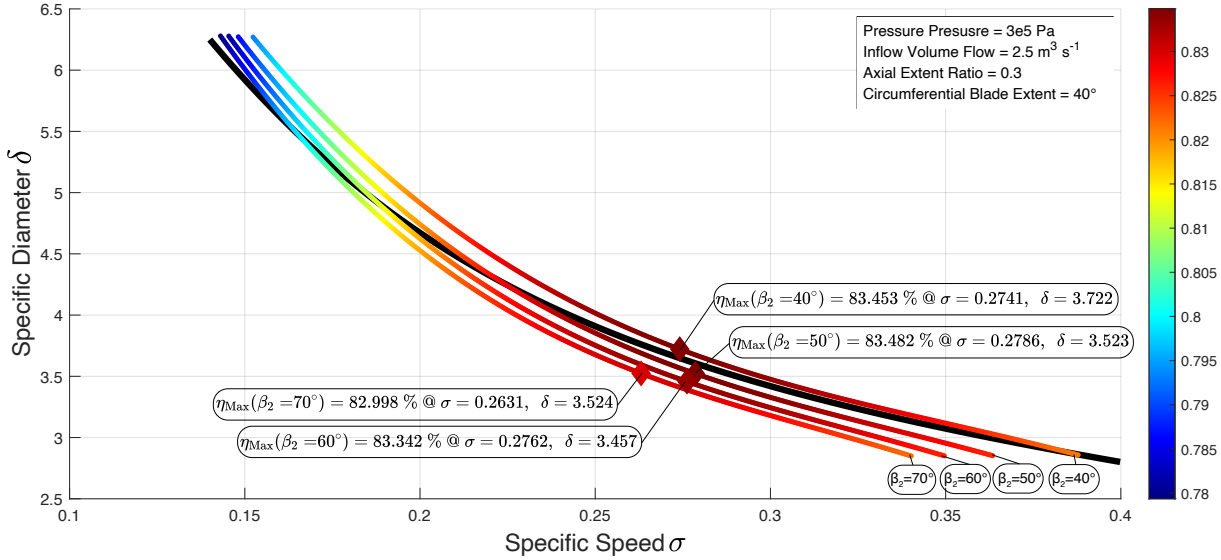

Figure 6: Duty-specific Cordier lines for a fixed duty with $\beta_2 = 40°$ to $70°$. The color represents the efficiency approximation. The original Cordier line is drawn in black color.

A simple optimization algorithm is used to identify a pair of specific speed σ and specific diameter δ, which will provide the best efficiency according to the underlying efficiency correlation. This is done for each duty-specific Cordier line. The efficiency values and the corresponding location in the Cordier diagram — pair of specific speed σ and specific diameter δ — of these optimized designs are shown as diamonds in Figure 6. It is noted that the efficiency values are very similar for different values of the relative blade angle β_2. However, as the other design values are fixed, no large deviations of the efficiency values were expected. Figure 7 (a) supports this. The influence of the location along the Cordier — represented by the specific speed σ — is considerably greater than the influence of the relative blade angle β_2.

The technique can also be applied to other compressor characteristics. As an example, the most efficient designs on several duty-specific Cordier lines for different β_2-values are identified. A normalized speed line width ($\dot{m}_{\mathrm{Norm}} = {\dot{m}_{\mathrm{Choke}} - \dot{m}_{\mathrm{Surge}}}/{\dot{m}_{\mathrm{Op}}}$) is plotted against the relative blade angle and interpolated by a third degree polynomial regression model (Figure 7 (b)). In this

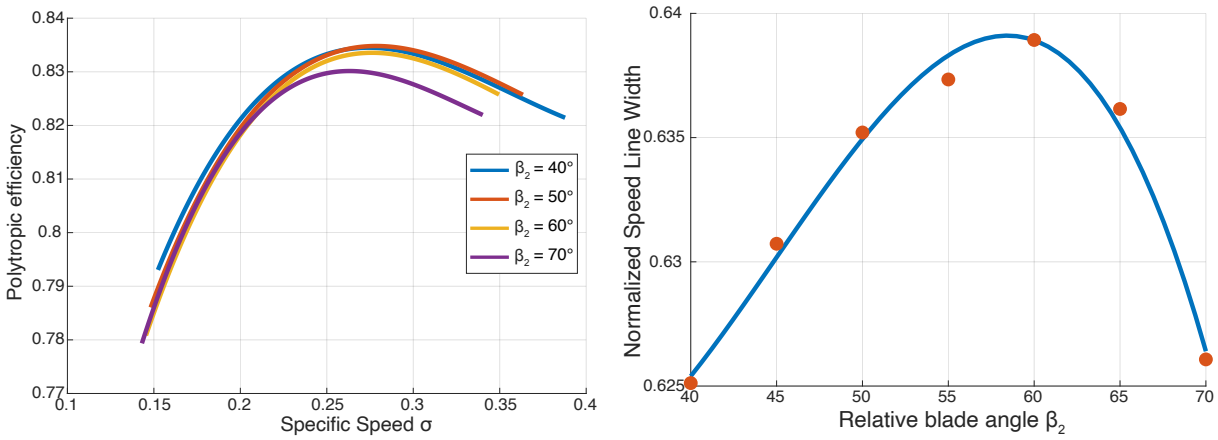

(a) (b)

Figure 7: Approximation of the efficiency along duty-specific Cordier lines for different values of β_2 against the specific speed σ (a); Approximation of the normalized speed line width $\dot{m}_{\mathrm{Norm}}$ for each duty-specific Cordier line's most efficient design against β_2 (b)

example, the user could use both plots to weight a high efficiency at low values of β_2 against a wider speed line around $\beta_2 = 60°$.

CONCLUSIONS

Duty-specific Cordier lines for radial turbocompressors were introduced to provide a more complete understanding of the compressor's machine design space.

Based on a two-level design of experiments, 50 compressor designs with 50 geometry variations each were simulated. Their maximum efficiency values were used to train a surrogate model, which approximates the efficiency of radial turbocompressors. The model's input parameters are all available at the start of the compressor's design process. It was compared with a well-established efficiency correlation. The results are plausible and indicate a higher underlying dimensionality. The model was implemented in the design workflow by providing duty-specific Cordier lines, which are generated for a specific set of design parameters.

The approach can be used to approximate the properties for every machine design combination inside the underlying design space. Given a suitable efficiency correlation, duty-specific Cordier lines may be created for any duty at the start of the design process with little computational effort. They can greatly enhance the designer's ability to make knowledge-based decisions while defining the turbocompressor's properties.

REFERENCES

Ansys Inc. (2022). *Ansys CFX Reference Guide: Release 2022 R2*.

Badawy, Mohammed F. et al. (2017). "Hybrid nonlinear surrogate models for fracture behavior of polymeric nanocomposites". In: *Probabilistic Engineering Mechanics* 50, pp. 64–75. DOI: 10.1016/j.probengmech.2017.10.003.

Casey, Michael and Chris Robinson (2021). *Radial Flow Turbocompressors*. Cambridge University Press.

Cordier, Otto (1953). "Ähnlichkeitsbedingungen für Strömungsmaschinen". In: *Brennstoff-Wärme-Kraft* 5.10, pp. 337–340.

Cumpsty, N A (1996). *Compressor aerodynamics*. Longman.

Fister, Werner (1986). *Fluidenergiemaschinen: Band 2: Auslegung, Gestaltung, Betriebsverhalten ausgewählter Verdichter- und Pumpenbauarten*. Springer Berlin Heidelberg. DOI: 10.1007/978-3-642-82524-8.

Geller, Marius, Christoph Schemmann, and Norbert Kluck (2017). "Optimization of the Operation Characteristic of a Highly Stressed Centrifugal Compressor Impeller Using Automated Optimization and Metamodeling Methods". In: *Volume 2C: Turbomachinery*. American Society of Mechanical Engineers. DOI: 10.1115/GT2017-63262.

Giuffre, Andrea, Piero Colonna, and Matteo Pini (2022). "The Effect of Size and Working Fluid on the Multi-Objective Design of High-Speed Centrifugal Compressors". In: *International Journal of Refrigeration* 143, pp. 43–56. DOI: 10.1016/J.IJREFRIG.2022.06.023.

Kim, J. H., J. H. Choi, A. Husain, and K. Y. Kim (2010). "Multi-objective optimization of a centrifugal compressor impeller through evolutionary algorithms". In: *Proceedings of the Institution of Mechanical Engineers, Part A: Journal of Power and Energy* 224.5, pp. 711–721. DOI: 10.1243/09576509JPE884.

Lataniotis, C, D Wicaksono, S Marelli, and B Sudret (2022). *UQLab user manual – Kriging (Gaussian process modeling)*. Tech. rep. Chair of Risk, Safety and Uncertainty Quantification, ETH Zurich.

Lattner, Yannick and Marius Geller (2023). "Radial Turbocompressor Chord Length Approximation for the Reynold's Number Calculation". In: *Fachhochschule Dortmund*. DOI: 10.26205/OPUS-3335.

Lattner, Yannick, Marius Geller, and Norbert Kluck (2022). "Generierung und Parametrisierung von Radialverdichterkennlinien auf Basis neuronaler Netze". In: *NAFEMS DACH Regionalkonferenz - Conference Proceedings*, pp. 287–292.

Lattner, Yannick, Marius Geller, and Michael Kutz (2023). "Physics-based surge point identification for unsupervised CFD-computation of centrifugal compressor speed lines". In: *Energy Conversion and Management: X* 17, p. 100337. DOI: 10.1016/j.ecmx.2022.100337.

Marelli, S et al. (2022). *UQLab user manual – Sensitivity analysis*. Tech. rep. Chair of Risk, Safety and Uncertainty Quantification, ETH Zurich.

Omidi, Mohammad et al. (2019). "Improving Centrifugal Compressor Performance by Optimizing the Design of Impellers Using Genetic Algorithm and Computational Fluid Dynamics Methods". In: *Sustainability* 11.19, p. 5409. DOI: 10.3390/su11195409.

Rodgers, C (1979). "Specific speed and efficiency of centrifugal impellers". In: *Performance prediction of centrifugal pumps and compressors*, pp. 191–200.

Rodgers, C. (1991). "The Efficiencies of Single-Stage Centrifugal Compressors for Aircraft Applications". In: *Volume 1: Turbomachinery*. American Society of Mechanical Engineers. DOI: 10.1115/91-GT-077.

Rusch, Daniel and Michael Casey (2012). "The Design Space Boundaries for High Flow Capacity Centrifugal Compressors". In: *Volume 8: Turbomachinery, Parts A, B, and C*. American Society of Mechanical Engineers, pp. 543–556. DOI: 10.1115/GT2012-68105.

Schemmann, Christoph (2019). "Optimization of Centrifugal Compressor Impellers by a Multifidelity Sampling Method Taking Analytical and Empirical Information into Account". PhD thesis. Bauhaus-Universität Weimar. DOI: 10.25643/BAUHAUS-UNIVERSITAET.3974.

Traupel, Walter (2001). *Thermische Turbomaschinen: Geänderte Betriebsbedingungen, Regelung, Mechanische Probleme, Temperaturprobleme*. Springer. DOI: 10.1007/978-3-642-17465-0.